Phase behavior of a model colloid-polymer mixture

S. M. Ilett, A. Orrock, W. C. K. Poon, and P. N. Pusey
Department of Physics and Astronomy, The University of Edinburgh, Mayfield Road, Edinburgh EH9 3JZ, United Kingdom
(Received 29 June 1994)

We report a detailed experimental study of a model hard-sphere colloid plus nonadsorbing polymer mixture in which the depletion effect causes phase separation. The key parameter that determines the topology of the phase diagram is the ratio $\xi = r_g/a$ of the radius of gyration (r_g) of the polymer molecules to the radius (a) of the colloidal particles. At small ξ, the addition of the polymer simply expands the colloidal fluid-crystal coexistence region of the pure hard-sphere system. For larger values of ξ, however, a three-phase coexistence of colloidal gas, liquid, and crystal phases is observed. The crossover between the two topologies is found at $\xi \sim 0.25$. These experimental observations are compared with the predictions of a recent statistical mechanical theory for such mixtures [Lekkerkerker *et al.*, Europhys. Lett. **20**, 559 (1992)]. The relevance of our results to the current debate about the conditions necessary for the existence of a "liquid" state is discussed.

PACS number(s): 82.70.Dd, 64.70.−p, 64.75.+g

I. INTRODUCTION

It is known from experiment (see, for example, [1–9]) that the addition of enough nonadsorbing polymers to a suspension of colloidal particles causes phase separation to occur. Exclusion, or depletion, of polymer molecules from the region between closely spaced particles leads to an effective interparticle attraction. A detailed understanding of this phase separation is of considerable technological importance — nonadsorbing polymers are often used as rheological modifiers in colloidal products. The study of polymer-induced phase separation of colloids can also give insights into fundamental questions in condensed matter science, such as the conditions required for the existence of a liquid-gas critical point.

In this paper we report a comprehensive study of the phase behavior of a model system of hard-sphere colloids plus nonadsorbing polymers — sterically stabilized colloidal polymethylmethacrylate (PMMA) and random coil polystyrene (PS) in cis-decahydronaphthalene (cis-decalin) at room temperature (19° − 23°). The PMMA particles themselves have been studied extensively in recent years and appear to behave like hard spheres [10–13]. PS is a well known and well characterized model polymer. It is found that the topology of the phase diagram depends sensitively on the ratio $\xi = r_g/a$ of the radius of gyration r_g of the polymer molecules to the radius a of the colloidal particles. At $\xi = 0.08$, the addition of polymer simply expands the colloidal fluid-crystal coexistence region of the pure hard-sphere system. For larger polymers $\xi = 0.25$ and 0.57, however, a three-phase coexistence of colloidal gas, liquid, and crystal phases is observed. Data for the smallest polymer ($\xi = 0.08$) have been reported before [14], but will be summarized in this work for completeness. We describe here in detail results for the two larger polymers. Brief accounts of this work have been presented elsewhere [15,16]. At the same time, Leal Calderon *et al.* [17] reported similar observations in mixtures of colloidal polystyrene plus hydroxyethyl cellulose. The relation of their observations to those in this work is discussed in detail below.

II. THEORETICAL BACKGROUND

The first theoretical interpretation of phase separation induced by a nonadsorbing polymer was due to Asakura and Oosawa [18], who discussed it in terms of the "depletion" effect (Fig. 1). Polymer molecules and colloidal particles are mutually impenetrable. Thus the center of a polymer molecule of radius r_g is excluded from a region of thickness of the order of r_g from the surface of each particle — the "depletion region". If the depletion regions of two particles overlap, there is an unbalanced osmotic pressure pushing the particles together, which can be expressed in the form of an attractive pair potential, the depletion potential, U_{dep} [19, 20]:

$$U_{dep} = \begin{cases} +\infty & \text{for } r \le \sigma \\ -\Pi_p V_{overlap} & \text{for } \sigma < r \le \sigma + 2r_g \\ 0 & \text{for } r > \sigma + 2r_g \end{cases}, \tag{1}$$

where $\sigma = 2a$ is the particle diameter and Π_p is the osmotic pressure of the polymer. $V_{overlap}$ is the volume of the overlapping depletion zones between two particles at an intercenter separation of r. Explicitly,

$$V_{overlap} = \left(1 - \frac{3r}{2\sigma(1+\xi)} + \frac{1}{2}\left[\frac{r}{\sigma(1+\xi)}\right]^3\right)\frac{\pi}{6}\sigma^3(1+\xi)^3, \tag{2}$$

where $\xi = r_g/a$ is the size ratio.

The form of Π_p, the polymer osmotic pressure, deserves some comment since it appears that the wrong expression for this quantity continues to be used in the literature. If we take the polymer solution to be ideal, then

$$\Pi_p = n_p^{(R)} k_B T. \tag{3}$$

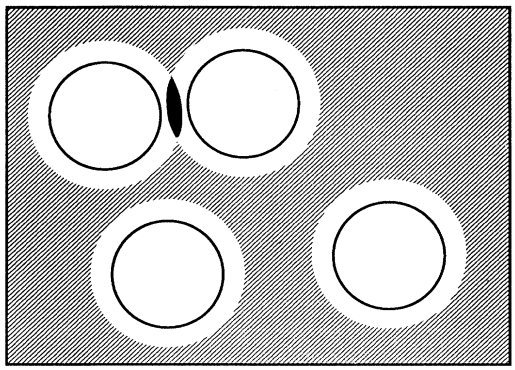

FIG. 1. Schematic illustration of depletion and free volume. Each particle is surrounded by a *depletion zone* (white); this is the region immediately next to each particle surface, which is inaccessible to the centers of polymer coils. The hatched area is the *free volume* V_{free}, which is available to centers of polymer coils. The relevance of the number density of polymer coils in the free volume $n_p^{(R)}$ is discussed in the text. The overlap of depletion zones (black) gives rise to extra free volume for the polymer and therefore a larger negative contribution to the entropic term of the free energy. This mechanism induces an effective attraction between the particles.

The polymer number density in this equation, $n_p^{(R)}$, can be interpreted in one of three equivalent ways.

(a) It is the number density of a polymer coils in a reservoir of pure polymer solution in osmotic equilibrium with the sample (which is a *mixture* of colloids and polymers) [21].

(b) Equivalently, $n_p^{(R)}$ is the number density of a polymer in the free volume V_{free} in the sample [22] (see Fig. 1):

$$n_p^{(R)} = \frac{N_p}{V_{free}}. \tag{4}$$

The free volume is the volume not occupied by colloidal particles or their associated depletion regions (see above) and N_p is the number of polymer coils in the sample. This can be written as a fraction of the sample volume V,

$$V_{free} = \alpha V \ , \tag{5}$$

where we have introduced the free-volume fraction α. At very low colloid volume fraction ϕ, $\alpha \approx 1 - \phi(1+\xi)^3$. A more accurate approximation is available through scaled particle theory (see explanation and references in [21, 22]):

$$\alpha = (1-\phi)\exp[-A\gamma - B\gamma^2 - C\gamma^3] \tag{6}$$

in which $\gamma = \phi/(1-\phi)$, $A = 3\xi + 3\xi^2 + \xi^3$, $B = 9\xi^2/2 + 3\xi^3$, and $C = 3\xi^3$ (ξ is the size ratio introduced above) [23].

(c) Finally, we can relate $n_p^{(R)}$ to the polymer chemical potential μ_p (which of course must be the same in the sample and the reservoir) [21],

$$\mu_p = k_B T \ln(n_p^{(R)} \lambda_p^3) \tag{7}$$

where λ_p is the de Broglie thermal wavelength for the polymer.

Note that the variable directly accessible to experiment is the number density of polymer molecules in the *sample volume* V:

$$n_p = \frac{N_p}{V}. \tag{8}$$

Equations (4) and (5) then tell us that n_p and $n_p^{(R)}$ are related via the free volume fraction α:

$$n_p = \alpha n_p^{(R)}, \tag{9}$$

so that

$$\Pi_p \neq n_p k_B T. \tag{10}$$

The right-hand side of Eq. (10) continues to be used by a number of authors in the calculation of the depletion potential. This is wrong by a factor of $1/\alpha$, which is significant at large size ratios and/or high colloid volume fractions.

The availability of an analytical form of U_{dep} allows a perturbation approach to predict the phase behavior of colloid-polymer mixtures [24]. The pair interaction between two colloid particles is written as

$$U(r) = U_0(r) + U_{dep}(r). \tag{11}$$

The behavior of the pure suspension under the influence of the interparticle potential U_0 (hard-sphere, Yukawa, etc.) is assumed to be known. The effect of the added polymer, entirely contained in U_{dep}, is then treated by thermodynamic perturbation theory. Using this approach with the form of U_{dep} given in Eq. (1) and U_0 as the hard-sphere potential, Gast *et al.* [24] predicted that the effect of added polymer depends crucially on the polymer-to-particle size ratio $\xi = r_g/a$. For a size ratio less than a crossover value $\xi < \xi_{co} \approx 0.3$, adding polymer merely expands the colloidal fluid-crystal coexistence region, which occurs at $0.494 < \phi < 0.545$ for a pure hard-sphere colloid [25, 10]. When $\xi > \xi_{co}$, a critical point appears in the phase diagram and a colloidal *liquid* phase becomes possible. Note that the use of U_{dep} in perturbation calculations has prompted a number of theoretical and simulational studies on the adequacy of the simple form given in Eq. (1), as well as the underlying assumption of pairwise additivity [26–29].

The forms of the phase diagrams predicted by the perturbative approach in [24] are similar to those shown in Figs. 2(a), 2(b), and 2(c) for the three size ratios $\xi = 0.08, 0.33$, and 0.57, respectively. The horizontal axes in these diagrams plot the colloid volume fraction ϕ. The vertical axes plot the effective volume fraction of polymer coils in a reservoir in osmotic equilibrium with the sample,

$$\eta_p^{(R)} = \frac{4}{3}\pi r_g^3 n_p^{(R)}, \tag{12}$$

where $n_p^{(R)}$ is the reservoir number density already introduced in Eq. (3). Reference to Eq. (7) then shows

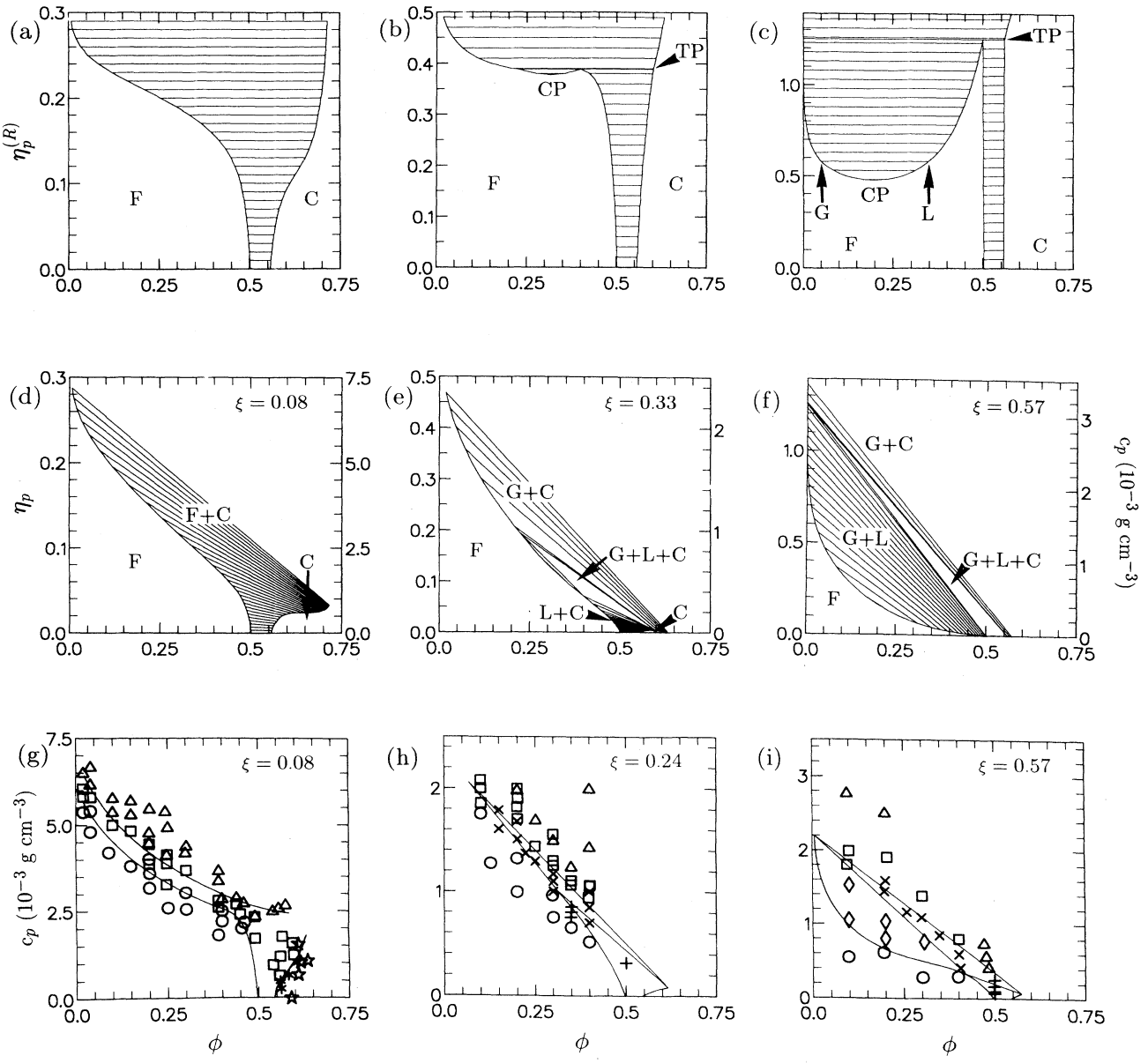

FIG. 2. (a)–(c) Theoretical phase diagrams, calculated according to the method in [22], plotted in the $(\phi, \eta_p^{(R)})$ plane for size ratios $\xi = 0.08$, 0.33, and 0.57. The horizontal axis is the colloid volume fraction ϕ and the vertical axis is the effective polymer volume fraction in a reservoir in osmotic equilibrium with the sample [$\eta_p^{(R)}$; see Eq. (12) in the text]. In (a) only the fluid, the fluid plus crystal, and the crystal are predicted. In (c) a region of gas-liquid coexistence is also predicted; the critical point and triple line are indicated. In (b) the critical point and triple line almost coincide. The symbols denote the following: CP, critical point; TP, triple line; F, fluid; G, gas; L, liquid; C, crystal; F+C, fluid plus crystal. (d)–(f) Theoretical phase diagrams, according to [22], in the (ϕ, η_p) plane for the same size ratios: the horizontal axis is again ϕ; the vertical axis plots the effective volume fraction of polymer molecules in the *sample* volume. Vertical axes in units of g per cm^3 are also given on the right of each figure to facilitate comparison with experimental data. The symbols are the same as in (a)–(c). (g)–(i) Experimental phase diagrams for size ratios $\xi = 0.08, 0.25$, and 0.57; the vertical axes plot the polymer concentration in g per cm^3. (g) is taken from [14]. All lines on (g)–(i) are drawn in as guides to the eye, except for the triangular regions in (h) and (i), which have been located with the aid of experimentally determined colloid concentrations in the three coexisting phases (see text). The symbols denote the following: circle, fluid; diamond, gas plus liquid; cross, gas plus liquid plus crystal; plus sign, liquid plus crystal; square, gas plus crystal; triangle, gel (for $\xi = 0.08$) or no visible crystallites (for $\xi = 0.33$ and 0.57); stars, glass.

that

$$\eta_p^{(R)} = \frac{4}{3}\pi \frac{r_g^3}{\lambda_p^3} e^{\mu_p/kT}. \quad (13)$$

The *horizontal* tie lines in the two-phase regions in this representation therefore indicate equal polymer chemical potentials in the two coexisting phases [30].

The $(\phi, \eta_p^{(R)})$ representation invites a direct comparison with the density-temperature phase diagram of an ordinary, atomic substance such as water, where the polymer reservoir volume fraction $\eta_p^{(R)}$ functions as an inverse temperature. In the $(\phi, \eta_p^{(R)})$ plane, three-phase coexistence [Figs. 2(b), and 2(c)] appears as a "triple line": the colloid volume fractions in the three coexisting phases are different, while the polymer chemical potential is constant throughout. One disadvantage of this representation is that the horizontal tie lines in two-phase regions give no direct indication of the likely occurrence of polymer partitioning upon phase separation. This has been pointed out by a number of authors recently [21, 31–33].

A more recent statistical mechanical approach [22] discusses phase behavior in terms of the free energy of the whole (colloid plus polymer) system rather than in terms of an effective attractive potential between colloid particles induced by the added polymer. A simple asymmetric nonadditive hard-sphere model is used for the mixture. The colloids are treated as hard spheres. The polymers are regarded as points, i.e. they do not interact with one another. But each point is excluded from coming closer than a distance δ from the surface of each hard sphere, thus modeling the excluded volume interaction between a polymer and a colloid. In a mean-field treatment of this model, the free energy separates into two parts

$$F_{total} = F_c(N_c, V) + F_p(N_p, V_{free}). \quad (14)$$

$F_c(N_c, V)$ is the free energy of N_c hard spheres in a volume V, while $F_p(N_p, V_{free})$ is the free energy of a perfect gas of N_p points confined to the free volume left for them by the hard spheres V_{free}. At high polymer concentration, the free energy of the mixture is minimized (or the entropy is maximized) by the formation of a dense colloidal phase in which the depletion zones of individual particles overlap, thus providing extra free volume for the polymer coils (Fig. 1). The calculations in [22] were performed in terms of the variables $(\phi, \eta_p^{(R)})$. Phase diagrams, however, were given in two representations, $(\phi, \eta_p^{(R)})$, where $\eta_p^{(R)}$ is the effective volume fraction of polymer molecules in the *reservoir* [already introduced in Eq. (12)], and (ϕ, η_p), where $\eta_p = (4/3)\pi r_g^3 n_p$ is the volume fraction of polymer molecules in the *sample*.

The $(\phi, \eta_p^{(R)})$ phase diagrams calculated by Lekkerkerker *et al.* [22] are almost identical to those plotted in the earlier work of Gast *et al.* [24] (see, however, [30]) and are given in Figs. 2(a) – 2(c) for three size ratios. However, the (ϕ, η_p) phase diagrams [Figs. 2(d)–(f)], which make the most direct contact with experiment, lead to *oblique* tie lines in all two-phase regions, giving a direct prediction of polymer partitioning between coexisting phases. Moreover, the three-phase coexistence at large size ratios now appears as a triple *region* rather than as a triple line: the volume fractions of the colloid and the polymer are different in the three coexisting phases [34]. The experimental data reported below make direct contact with the phase diagrams presented in the (ϕ, η_p) representation in Figs. 2(d)–2(f). The predictions of this theory have also been compared in some detail with a recent computer simulation [35].

III. EXPERIMENT

The particles used in this study consisted of PMMA cores, stabilized sterically by thin, 10 – 15 nm, chemically grafted layers of poly-12-hydroxystearic acid [36]. They were suspended in cis-decahydronaphthalene (cis-decalin). Suspensions of this type have been studied extensively with emphasis on phase behavior [10], particle dynamics [11], crystallization [12], and glass formation [13]. These studies have established that the interparticle interaction is steep and repulsive and is well approximated by that of hard spheres. Samples were made by dilution or concentration of a stock solution. As described previously [10], the effective hard-sphere volume fractions ϕ of the samples were calculated using literature values of the densities $\rho_{PMMA} = 1.18$ gcm^{-3} and $\rho_{decalin} = 0.894$ gcm^{-3} and scaled so that freezing occurs at the hard sphere value $\phi = 0.494$. The particle radii were determined by dynamic light scattering to be $a = 217$ and 228 nm (see Table I). Their polydispersities, also determined by dynamic light scattering [37], were of the order of 5%.

Polystyrene in cis-decalin ($T_\theta = 12.5\,^\circ$C) is a well studied system [38]. In our earlier work [14], the results of which are also summarized below, polystyrene from Pressure Chemical Company with $M_w = 0.39 \times 10^6 (M_w/M_n < 1.10$, polymer $A)$ was used, which gave a size ratio of $\xi \approx 0.08$ at 19 °C. Two sizes of polymer from Polymer Laboratories were used in this work, with molecular weights $2.85 \times 10^6 (M_w/M_n < 1.30$, polymer $B)$ and $14.4 \times 10^6 (M_w/M_n = 1.21$, polymer $C)$. Data in the literature [38] enable us to estimate the radii of gyration at 23 °C to be $r_g \approx 54$ nm and $r_g \approx 130$ nm, respectively. Thus the size ratios were $\xi \approx 0.24$ (polymer B) and $\xi \approx 0.57$ (polymer C).

Samples were prepared by mixing PMMA suspensions with PS stock solutions. Each sample was then homogenized by prolonged tumbling. In this work (with polymers B and C), the temperature was controlled at $23 \pm 0.1\,^\circ$C using a recirculating bath. In the previous work (with polymer A), observations were made at room temperature, $19 \pm 2\,^\circ$C. Extensive studies were carried out on samples covering a wide range of (ϕ, c_p) values.

Samples were inspected visually at regular intervals. The samples were sufficiently translucent that processes, such as crystallization, occurring in the bulk could be seen.

IV. RESULTS AND DISCUSSION

The different kinds of phase behavior observed are summarized in Figs. 2(g)–2(i). At low polymer con-

centrations for any of the three polymers, samples with $\phi < 0.494$ remained in single phases and appeared homogeneous, with a "fluidlike" arrangement of colloidal particles. The sequence of events upon further addition of polymer depends critically on the size ratio.

In samples with higher concentrations of polymer A [Fig. 2(g)], colloidal fluid-crystal coexistence was observed. Colloidal crystallites began to be visible a few hours after mixing. Nucleation appeared to be homogeneous throughout the sample volumes. Within a day or so the crystallites settled under gravity, leaving supernatant colloidal fluid separated from the polycrystalline phase by well defined boundaries. Crystallization was not observed, however, at even high polymer concentrations. Instead, samples exhibited metastable "gel" states, which have been described elsewhere [39, 40].

Higher concentrations of polymer B [Fig. 2(h)] gave samples showing three-phase coexistence. In such a sample, a diffuse meniscus separating two amorphous phases appeared a few hours after mixing, together with iridescent specks of nucleating colloidal crystallites throughout the sample. Over a day or so, these crystallites sank to the bottom, forming an iridescent layer of polycrystalline material. The meniscus separating the two amorphous phases also sharpened over the same time span. Preliminary dynamic light scattering showed that the particles in these two phases were mobile. We therefore identify the upper, less turbid, phase as a colloidal gas and the middle, more turbid phase, as a colloidal liquid. Still higher concentrations of polymer B gave samples showing colloidal gas-crystal coexistence. Figure 3 shows the visual appearance of samples exhibiting each of these three kinds of behavior.

Samples where the larger polymer C was added [Fig. 2(i)] showed similar behavior to samples with polymer B, except that a two-phase region of colloidal gas-liquid coexistence intervened between the single-phase fluid region and the three-phase coexistence region.

For both polymers B and C, the size of crystals in the crystal-fluid coexistence region was observed to decrease dramatically at increasing polymer concentrations. At the highest polymer concentrations, no iridescence was observed in the dense sediment in samples which were expected to show a gas-crystal coexistence; if any colloidal crystallites existed, their sizes would be less than ≈ 0.03 mm. Pending a detailed investigation of phenomenology and light scattering behavior, it is unclear at present whether these observations point to the existence of a gelation transition analogous to the case of polymer A.

The compositions of coexisting colloidal gas, liquid, and crystal phases of any sample in the three-phase region are given by the vertices of the three-phase triangle. The phase volumes are determined by an extension of the lever rule [41]. We determined the volume fraction of colloidal particles in the three coexisting phases for both polymer B and polymer C. For the crystalline phase, this was done by measuring the position of the Bragg reflection due to the stacking of close-packed planes [12]. Colloidal gas and liquid phases were separated and dried down for the determination of mass fractions. The mass fractions were then converted to volume fractions by comparing to the mass fraction of a sample of pure colloid of known concentration. The results are presented in Table II.

Each set of three numbers can be checked for internal consistency by appealing to the conservation of mass. The measured fractions of the phases in a three-phase sample f_{gas}, f_{liq}, and f_{cryst} have to satisfy the following relation:

$$f_{gas}\phi_{gas} + f_{liq}\phi_{liq} + f_{cryst}\phi_{cryst} = \phi_0, \tag{15}$$

where ϕ_0 is the initial concentration of a colloid in the sample. This was found to be the case within experimental errors in each case. A triangular region of the three-phase coexistence consistent with the measured values of $(\phi_{gas}, \phi_{liq}, \phi_{cryst})$ and the observed behavior of samples in each case [42] has been included in the data plots in Figs. 2(h) and 2(i).

The sequence of observed behavior (with the exception of the "gel" state) reported above clearly provides broad confirmation of the predictions of the theory in [22]. In particular, it is interesting that we did not observe a colloidal gas-liquid coexistence with polymer B, which nevertheless gave rise to samples showing three-phase coexistence. This is precisely the behavior predicted by the theory of Lekkerkerker *et al.* [22] for a system with size ratio ξ close to but greater than the crossover size ratio ξ_{co}. Figure 2(e) shows that when ξ is just above ξ_{co}, the three-phase region is already well developed, while the liquid-gas coexistence region is extremely narrow. The latter region, however, grows dramatically in extent as ξ increases further [Fig. 2(f)]. The theoretical work of both Gast *et al.* [24] and Lekkerkerker *et al.* [22] predict that $\xi_{co} \approx 0.3$. Our results for polymer B suggest that, in our system, ξ_{co} is closer to 0.25. The large area of the gas-liquid coexistence in the phase diagram with polymer C ($\xi = 0.57$) is in line with this interpretation.

The colloid concentrations of the three coexisting phases at $\xi = \xi_{co}$ can be compared. Theory at $\xi = 0.33$ gives $(\phi_{gas}, \phi_{liq}, \phi_{cryst}) = (0.22, 0.40, 0.60)$, while at the experimental crossover size ratio of $\xi = 0.25$ we measure $(\phi_{gas}, \phi_{liq}, \phi_{cryst}) = (0.07, 0.31, 0.61)$. The agreement is good for ϕ_{cryst}, satisfactory for ϕ_{liq}, but poor for ϕ_{gas}. Note, however, that ϕ_{gas} is a very sensitive function of ξ

TABLE I. Particles and polymers used in this work.

Particle radius a (nm)	Polymer	$10^{-6}M_w$	Radius of gyration r_g (nm)	Size ratio
217	A	0.39	18 (19°C)	0.08
228	B	2.85	54 (23°C)	0.24
228	C	14.4	130 (23°C)	0.57

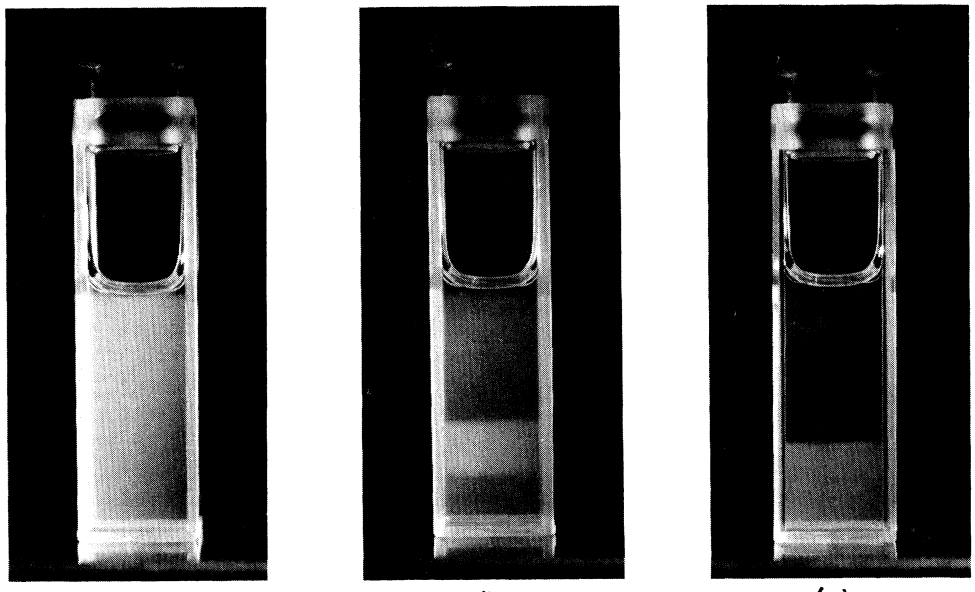

FIG. 3. The appearance of three samples at $\phi = 0.2$ with increasing concentrations of polymer B. Sample (a) is in the single-phase fluid region of the phase diagram. Sample (b) has separated into coexisting crystal (bottom), liquid (middle), and gas (top) phases, while sample (c) has coexisting crystal (bottom) and gas (top) phases. To the naked eye, the bottom phase in both (b) and (c) showed iridescence. (For photographic purposes, these samples were prepared in a mixture of cis-decalin and tetralin which matches the refractive index of the PMMA particles. This has the effect of shifting all the phase boundaries to slightly lower polymer concentrations due to a small expansion in polymer coil radius.)

near ξ_{co} (see Fig. 4). For example, a small increase of the size ratio from $\xi = 0.33$ to $\xi = 0.35$ lowers the predicted volume fraction of the coexisting gas from $\phi_{gas} = 0.22$ to $\phi_{gas} = 0.13$. Too much should not, therefore, be made of the appararent poor disagreement between the theoretical and experimental values of ϕ_{gas} at ξ_{co}.

The changes in concentrations of the coexisting gas, liquid, and crystal phases at increasing ξ predicted by the approach in [22] are plotted in Fig. 4. As ξ increases from ξ_{co}, ϕ_{gas} decreases dramatically, ϕ_{liq} increases slightly, and ϕ_{cryst} decreases slightly. All of these trends are confirmed by our measurements. The large decrease in ϕ_{gas} was a very visible effect; the topmost phase in a three-phase sample with polymer B was distinctly turbid, while the corresponding phase in a three-phase sample with polymer C was almost clear.

Although the overall pattern of behavior at increasing sizes of polymer predicted by the theory of Lekkerkerker *et al.* [22] has been confirmed in this work, there is clearly some disagreement in matters of detail. This is not surprising since the theory is a mean-field approximation and the polymer is treated by a simple model. (A more detailed discussion of the limitations of the theory in [22] can be found in that reference, as well as in [14].)

Recently Leal Calderon *et al.* [17] have reported observations similar to those discussed in this work. These authors studied mixtures of hydroxyethyl cellulose with charged colloidal polystyrene particles at the approximate size ratios of $\xi = 0.21, 0.25$, and 0.30. Although these authors published no data points, we can compare and contrast their observations with those reported here in a number of ways. Qualitatively, Leal Calderon *et al.* observed three-phase coexistence in samples with $\xi = 0.25$ and 0.30, but not in samples with $\xi = 0.21$. These results, together with those reported in this work, put it beyond doubt that the occurrence of a critical point in the phase diagram of a colloid plus nonadsorbing polymer-to-mixture is crucially dependent on a large enough polymer-to-colloid size ratio. However, the liquid-gas coexistence region at $\xi = 0.25$ was apparently already well developed in [17] and the colloid volume fraction in the coexisting gas phase in a three-phase sample was already very low, $\phi_{gas} \approx 0.04$. Very probably these differences point to the important role of polymer nonideality in determining the details of the phase diagram [43]. There is also apparently a difference in the kinetics

TABLE II. Compositions of coexisting gas, liquid, and crystal phases.

Polymer	Size ratio	ϕ_{gas}	ϕ_{liq}	ϕ_{cryst}
B	0.24	0.070 ± 0.005	0.31 ± 0.02	0.615 ± 0.006
C	0.57	0.0055 ± 0.0002	0.44 ± 0.02	0.574 ± 0.007

of phase separation in the case of three-phase coexistence. Crystallization in our system appears to proceed homogeneously throughout a mixture that is simultaneously separating into gas-liquid phases. Leal Calderon *et al.*, however, reported that "the sediment is formed first and a solid phase starts to grow after several days or weeks." The distinction between "sediment" and "solid phase" is unclear. Also these authors did not mention the existence of any metastable states at high polymer concentrations.

V. CONCLUDING REMARKS

Besides being an observation of three-phase coexistence in a colloid-polymer system, the results reported here have wider significance for condensed matter science. Much progress has been made in the past three decades in the understanding of the liquid-gas critical point [44]. Nevertheless, the prior question of what conditions are required for the *existence* of a critical point, and therefore of a genuine liquid state, has only been poorly addressed theoretically and experimentally alike. Indeed, it seems to have been a common assumption until very recently that any amount of attraction added to the hard-sphere potential will produce a critical point in the phase diagram.

For instance, much effort has been devoted to studying gas-liquid coexistence in the Baxter adhesive hard-sphere (AHS) model (see, e.g., [45] and references therein). The AHS potential consists of the hard-sphere potential plus a "stickiness" term at contact of the form $k_BT \ln[12\tau\delta(r-\sigma)/\sigma]$, where τ is the Baxter stickiness parameter and δ is the Dirac delta function. Stell [46] has recently argued that the only likely thermodynamically stable states in this system are the fluid and crystal states. The results of recent density functional thoery calculations (see, e.g.,[47]) also suggest strongly that this may indeed be so, i.e., that the gas-liquid coexistence curve in the AHS system is "buried" inside the fluid-crystal coexistence region [48]. Thus the AHS liquid-gas critical point studied by numerous investigators is in fact probably *metastable*.

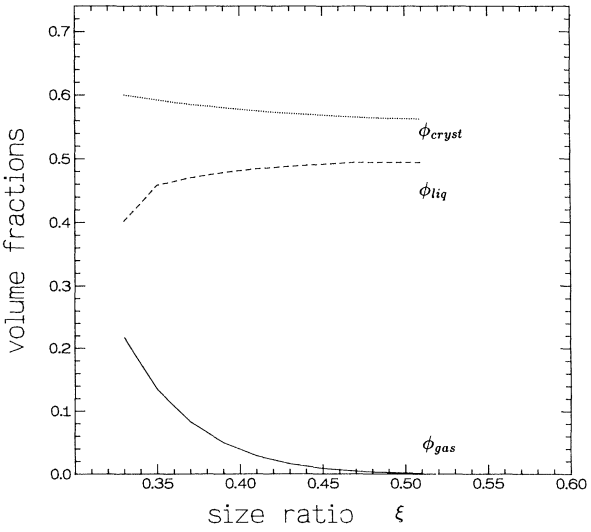

FIG. 4. The concentrations of coexisting gas, liquid, and crystal phases predicted by the theory of Lekkerkerker *et al.* [22] at size ratios from $\xi = \xi_{co} \approx 0.32$ upward.

Theoretical results on colloid-polymer mixtures such as those in [24, 22], as well as recent simulations of fullerene (C_{60}) [49, 50] and a model Yukawa system [51], suggest that *an attractive potential of sufficiently long range* is necessary for the existence of a thermodynamically stable liquid-gas critical point. The experimental results presented here provide significant confirmation of this prediction and a quantitative measurement of the critical potential range, namely, of the order of $0.25\times$ the hard-sphere diameter. Previous work on the effect of temperature on the phase diagram at the size ratio $\xi = 0.08$ [14] indicates, however, that the nonideality of the polymer can have subtle secondary effects (see also [43]). The theoretical approach of Lekkerkerker *et al.* [22] can, in fact, be modified to include temperature effects up to the second virial coefficient of the polymer. The modified theory then predicts that a phase diagram with the crossover topology, viz., a well developed three-phase region, but a very small gas-liquid region [Fig. 2(e)], persists over a range of temperatures for a suitable choice of polymer. Details of this will be the subject of a forthcoming paper [52]. Nevertheless, it is already clear that the colloid-to-polymer size ratio is the dominant but not the only effect determining phase diagram topology in this system.

At present the physical reason why the range of the potential should be an important factor in giving rise to a critical point is far from clear. Computer simulation is one way to gain some physical insight. Further experimental work on the colloid plus polymer system used in this work is also in progress. For example, preliminary work has shown that the phase diagram is very sensitive to temperature [14, 52]. It is possible, therefore, that the abrupt change of topology as the size ratio increases past ξ_{co} could be brought about by temperature, allowing a detailed study of the manner in which a stable liquid-gas critical point emerges. Finally, it will also be necessary to seek to understand the reason why both the models in [24, 22] predict the same ξ_{co}, which is apparently too high.

ACKNOWLEDGMENTS

This work is supported by the UK Agriculture and Food Research Council. Some of the equipment used was purchased by funds made available by the Royal Society of London. Particles used in this work were kindly provided by Professor R. H. Ottewill and Dr. S. M. Underwood. We thank Professor H. N. W. Lekkerkerker for valuable discussions at various stages of this work and for drawing our attention to the references cited in [34, 46, 48]. We also thank Dr. P. B. Warren of Unilever Research Port Sunlight for the use of computer programs for producing Figs. 2(a)–(f) and for generating the data plotted in Fig. 4.

[1] H. de Hek and A. Vrij, J. Colloid Interface Sci. **79**, 289 (1981).
[2] C. Pathmamanoharan, H. de Hek, and A. Vrij, Colloid Polymer Sci. **259**, 769 (1981).
[3] P. R. Sperry, J. Colloid Interface Sci. **99**, 97 (1984).
[4] A. P. Gast, W. B. Russel, and C. K. Hall, J. Colloid Interface Sci. **109**, 161 (1986).
[5] B. Vincent, J. Edwards, S. Emmett, and R. Croot, Colloids Surf. **31**, 267 (1988).
[6] P. D. Patel and W. B. Russel, J. Colloid Interface Sci. **131**, 192 (1989).
[7] C. Smits, J. S. van Duijneveldt, J. K. G. Dhont, and H. N. W. Lekkerkerker, Phase Transitions **21**, 157 (1990).
[8] C. Smit, B. van der Most, J. K. G. Dhont, and H. N. W. Lekkerkerker, Adv. Colloid Interface Sci. **42** 33 (1992).
[9] A. J. Fillery-Travis, P. A. Bunning, D. J. Hibberd, and M. M. Robins, J. Colloid Interface Sci. **159**, 189 (1993).
[10] P. N. Pusey and W. ven Megen, Nature **320**, 340 (1986).
[11] W. van Megen, R. H. Ottewill, S. M. Owens, and P. N. Pusey, J. Chem. Phys. **82**, 508 (1985).
[12] P. N. Pusey, W. van Megen, P. Bartlett, B. J. Ackerson, J. G. Rarity, and S. M. Underwood, Phys. Rev. Lett. **63**, 2753 (1989).
[13] W. van Megen and P. N. Pusey, Phys. Rev. A **43**, 5429 (1991).
[14] W. C. K. Poon, J. S. Selfe, M. B. Robertson, S. M. Ilett, A. D. Pirie, and P. N. Pusey, J. Phys. II **3**, 1075 (1993).
[15] S. M. Ilett, W. C. K. Poon, P. N. Pusey, A. Orrock, M. K. Semmler, and S. Erbil, Prog. Colloid Polymer Sci. (to be published).
[16] P. N. Pusey, W. C. K. Poon, S. M. Ilett, and P. Bartlett, J. Phys. Condensed Matter **6**, A29 (1994).
[17] F. Leal Calderon, J. Bibette, and J. Biais, Europhys. Lett. **23**, 653 (1993).
[18] S. Asakura and F. Oosawa, J. Chem. Phys. **22**, 1255 (1954).
[19] S. Asakura and F. Oosawa, J. Polymer Sci. **33**, 183 (1958).
[20] A. Vrij, Pure Appl. Chem. **48**, 471 (1976).
[21] H. N. W. Lekkerkerker, Colloid Surf. **51**, 419 (1990).
[22] H. N. W. Lekkerkerker, W. C. K. Poon, P. N. Pusey, A. Stroobants, and P. B. Warren, Europhys. Lett. **20**, 559 (1992).
[23] This expression for α derived from a theory of the fluid state should *not*, in principle, be used for working out the free volume fraction for any state with long-range order. The inaccuracies involved in using this expression for the hard-sphere solid, as in the work of Lekkerkerker *et al.* [22], have been discussed recently in [35].
[24] A. P. Gast, C. K. Hall, and W. B. Russel, J. Colloid Interface Sci. **96**, 251 (1983).
[25] W. G. Hoover and F. H. Ree, J. Chem. Phys. **49**, 3609 (1968).
[26] G. J. Fleer and J. M. H. M. Scheutjens, Adv. Colloid Interface Sci. **16**, 341 (1982).
[27] M. R. Shaw and D. Thirumalai, Phys. Rev. A **44**, 4797 (1991).
[28] E. J. Meijer and D. Frenkel, Phys. Rev. Lett. **67**, 1110 (1991).
[29] R. Dickman and A. Yethiraj, J. Chem. Phys. **100**, 4683 (1994).
[30] It is not clear that the variable ϕ_3 in Ref. [24] is equal to our $\eta_p^{(R)}$. The most natural interpretation of that paper suggests that $\phi_3 = (4/3)\pi r_g^3 n_p = \eta_p$ in our notation, in which case the phase diagrams should have looked more like the ones shown in Figs. 2(d), 2(e), and 2(f). This certainly is how subsequent authors have interpreted [24], leading to the use of $\Pi_p = n_p k_B T$ in calculating the depletion potential, which is wrong.
[31] E. Canessa, K. J. Grimson, and M. Silbert, Mol. Phys. **67**, 1153 (1989).
[32] M. M. Santore, W. B. Russel, and R. K. Prud'homme, Macromolecules **22**, 1317 (1989).
[33] P. N. Pusey, in *Liquids, Freezing and the Glass Transition*, edited by J. P. Hansen, D. Levesque, and J. Zinn-Justin (Elsevier, Amsterdam, 1991), Chap. 10.
[34] Compare M. Planck, *Treatise on Thermodynamics*, 3rd ed. (Dover, New York, 1926), Sec. 189, where it is shown that the triple point of the conventional p-T phase diagram of a simple substance becomes a triple region in the specific volume-specific energy representation. See the very illuminating discussion on the topology of phase diagrams plotted using different kinds of thermodynamic variables by Robert T. De Hoff, *Thermodynamics in Material Science* (McGraw-Hill, New York, 1993), Sec. 7.6 and 9.4.
[35] E. J. Meijer and D. Frenkel, J. Chem. Phys. **100**, 6873 (1994).
[36] L. Antl, R. D. Hill, R. H. Ottewill, S. M. Owens, S. Papworth, and J. A. Waters, Colloid Surf. **17**, 67 (1986).
[37] P. N. Pusey and W. van Megen, J. Chem. Phys. **80**, 3513 (1984).
[38] G. C. Berry, J. Chem. Phys. **44**, 4550 (1966).
[39] P. N. Pusey, A. D. Pirie, and W. C. K. Poon, Physica A **201**, 322 (1993).
[40] M. D. Haw, W. C. K. Poon, and P. N. Pusey, Physica A **208**, 8 (1994).
[41] P. Bartlett, J. Phys. Condens. Matter **2**, 4979 (1990); see also Robert T. De Hoff, *Thermodynamics in Material Science* (Ref. [34]).
[42] We did not attempt to determine the concentrations of polymer in the various phases, although this could, in principle, be done using the method outlined in the Appendix in [14].
[43] A very dramatic illustration of the effect of "nonideality" is provided by the recent work on the phase diagram of a mixture of hard spheres with a size ratio of 0.58: P. Bartlett, R. H. Ottewill, and P. N. Pusey, Phys. Rev. Lett. **68**, 3801 (1992) (experiment); M. D. Eldridge, P. A. Madden, and D. Frenkel, Nature **365**, 35 (1993) (simulation). This size ratio is almost exactly the same as that given by polymer C in this work. At 23 °C, the Fixman parameter for this polymer in cis-decalin [38] is 1.25, fairly nonideal, but very far from being hard-sphere-like. The phase diagram for this case, Fig. 2(i), is very different from those obtained for the hard-sphere mixture at practically an identical size ratio in the two references quoted. Compare also W. C. K. Poon and P. B. Warren, Europhys. Lett. **28**, 513 (1994).
[44] J. V. Sengers and J. M. H. Levelt Sengers, Annu. Rev. Phys. Chem. **37**, 189 (1986).
[45] W. G. T. Kranendonk and D. Frenkel, Mol. Phys. **64**, 403 (1988).
[46] G. Stell, J. Stat. Phys. **63**, 1203 (1991).
[47] See D. W. Marr and A. P. Gast, J. Chem. Phys. **99**, 2024 (1993), and references therein.
[48] The possibility of such a situation, of which many investigators seem unaware, has already been pointed out by

Cahn in 1968; see W. Cahn, Trans. Metallur. Soc. AIME **242**, 166 (1968). Figure 6 of this review referred to "a miscibility gap that is entirely metastable."

[49] A. Cheng, M. L. Klein, and C. Caccamo, Phys. Rev. Lett. **71**, 1200 (1993).

[50] M. H. J. Hagen, E. J. Meijer, G. C. A. Mooij, D. Frenkel, and H. N. W. Lekkerkerker, Nature **365**, 425 (1993).

[51] M. H. J. Hagen and D. Frenkel, J. Chem. Phys. **101**, 4093 (1994).

[52] P. B. Warren, S. M. Ilett, M. K. Semmler, and W. C. K. Poon (unpublished).

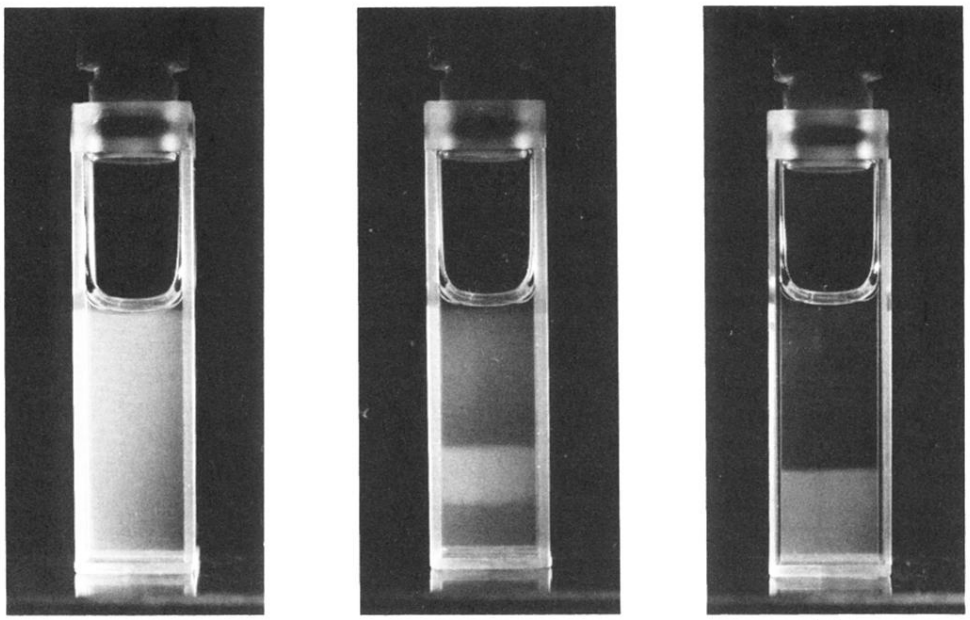

FIG. 3. The appearance of three samples at $\phi = 0.2$ with increasing concentrations of polymer B. Sample (a) is in the single-phase fluid region of the phase diagram. Sample (b) has separated into coexisting crystal (bottom), liquid (middle), and gas (top) phases, while sample (c) has coexisting crystal (bottom) and gas (top) phases. To the naked eye, the bottom phase in both (b) and (c) showed iridescence. (For photographic purposes, these samples were prepared in a mixture of cis-decalin and tetralin which matches the refractive index of the PMMA particles. This has the effect of shifting all the phase boundaries to slightly lower polymer concentrations due to a small expansion in polymer coil radius.)